



ARTICLE

Preparation of Porous Materials Derived from Waste Mussel Shell with High Removal Performance for Tableware Oil

Yi Yang¹, Zhaodi Wu¹, Lili Ji², Shiyao Lu², Hua Jing², Jiaying Sun², Jian Guo¹, Wendong Song³, Yaning Wang² and Lu Cai^{4,*}

¹College of Food and Medical, Zhejiang Ocean University, Zhoushan, 316022, China

²National Marine Facilities Aquaculture Engineering Technology Research Center, Zhejiang Ocean University, Zhoushan, 316022, China

³College of Petrochemical and Energy Engineering College, Zhejiang Ocean University, Zhoushan, 316022, China

⁴Donghai Science and Technology College, Zhejiang Ocean University, Zhoushan, 316000, China

*Corresponding Author: Lu Cai. Email: lucai89@126.com

Received: 26 January 2021 Accepted: 23 March 2021

ABSTRACT

In this work, carbonized mussel shell powder (CMSP) was modified by alkyl polyglucosides (APG) and rhamnolipid (RL) to render porous biomass a lipophilic surface, which was innovatively utilized as an environmentally friendly tableware cleaning material. The modified method was two-step hydrotherm-assisted synthesis. A contact angle meter was used to determine the surface hydrophobic property of modified samples (MTAR). The pore and the surface structure of CMSP and MTAR were characterized by BET, SEM, XRD, FTIR and XPS. The effect of removing oil was tested by gravimetric method. The results showed that the surface of MTAR was more porous and fluffier than CMSP, and the specific surface area is increased by 16.76 times. The results showed that when calcining CMSP at 1000°C, the oil removal rate of the synthesized MTAR is the best, and the decontamination rate can reach 87.05%. This research aims to develop a green and environmentally-friendly tableware cleaning material, solve environmental problems, and make full use of waste, which is very conducive to environmental protection.

KEYWORDS

Calcined mussel shell; modified; tableware cleaning; surfactant

1 Introduction

Nowadays, dishwashing detergent has become an essential commodity in our daily life, which could keep a clean kitchen environment. Usually, a typical dishwashing detergent consists of surfactants, builders, emulsifiers and a few additives [1], which are basically chemicals, they can affect human health and cause environmental pollution [2,3]. More seriously, long-term ingestion or exposure to these ingredients will cause the accumulation of chemical toxins in the body, reduce the concentration of calcium ions in the body's blood, acidify the blood, reduce the detoxification function of the liver, and increase liver cell disease, which is easy to induce cancer [4–7]. Currently, natural ingredients are becoming a new trend in the detergent industry due to their environmentally friendly, low cost and easily



degradable, such as saponins [8], pineapple by-product [9], sapindus mukorossi [10], etc. However, few natural ingredients are used in dishwashing detergent products, and the main ingredients of commercial detergents are still chemicals.

The common components of household and municipal sewage consist of surfactants and other components of detergents. They will enter the environment through the sewage system and cause harm to aquatic organisms [11,12]. In addition, detergent ingredients can interact with other substances in the water, causing toxicity and biodegradation [13]. Therefore, how to develop new cleaning materials (degradable, pollution-free, and healthy) is a scientific problem that needs to be solved urgently.

In recent years, bio-based porous materials have attracted widespread attention from researchers due to their abundant holes, excellent adsorb ability, non-toxicity, renewability and favorable stability, which have been applied in many fields, such as dye wastewater treatment [14], heavy metal removal [15], oil adsorption [16], etc. Among these, oil adsorption by bio-based porous materials has received much more attention. For example, Zhao et al. [17] used waste peanut shells to prepare a biodegradable and super-wet separation layer, which plays a very good role in oil-water separation. Xu et al. [18] used corn cobs and willows as materials, first coagulated and precipitated the biomass solution with water, then freeze-dried to obtain porous materials. These materials had effective adsorption capacity for methylene and oil. And a green sorbent porous material was prepared with natural rubber and reduced graphene oxide, which was used in the treatment of marine oil spills [19]. JO et al. [20] treated corncobs with acetic anhydride, which enhanced its hydrophobicity and had good adsorption to crude oil. However, to the best of our knowledge, the application of bio-based porous materials in the dishwashing detergent has not been reported yet.

Mussel shells are by-products of aquatic processing, accounting for about 70% of the biological weight of mussels. Every year, a large number of shells are stacked in farmland or embankments as solid waste, which not only occupies land resources, but also has a negative impact on the environment [21]. Under the control of biological genetics, mussel shells present a “brick-mud” assembly structure that cannot be synthesized by humans. In our previous studies, mussel shells have been prepared into various bio-based materials as oil pollution adsorbent [22], photocatalyst carrier and photo catalyst [23], where mussel shell porous material displays superior adsorption, dispersion, porousness and non-toxicity.

The purpose of this article is to use mussel shells as raw materials to obtain porous framework materials by carbonization, and use this as a matrix to modify them with alkyl polyglucosides (APG) and rhamnolipid (RL). Template method [24], chemical vapor deposition [25], hydrothermal [26] as well as chemical activation [27] are widely used processes to synthesize porous framework materials. In recent years, other new methods have been studied; Wang et al. [28] used freeze-drying method to prepare chitosan hybrid sponge. Carbonization of biomass raw materials through high temperature pyrolysis is also one of the methods [29,30]. Because it is calcined in the absence of oxygen, the carbon in the biomass does not undergo a combustion process, and the resulting products include pyrolysis gas, bio-oil and bio-char. Among them, the more valuable biochar is a black solid, which has the advantages of porosity, light weight and high stability. In addition, other methods have some specific requirements for raw materials. Carbonization can use many different types of feedstock, including agricultural waste, wood, animal manure, etc. Hence, carbonization can be a waste-to-resource process, this is also a good realization of the value-added utilization of agricultural waste.

As an emerging nonionic surfactant, APG possesses the advantage of low toxicity, high biodegradability and good ecological compatibility [31]. The raw materials come from natural renewable resources, are non-toxic and harmless, have excellent decontamination ability, and have a good synergistic effect with other surfactants. In the 1920s, APG has been reported. It is now widely used in household detergents, cosmetics and agricultural products [32]. RL is biodegradable, show low aquatic toxicity and can be produced from renewable resources [33]. As a bio-surfactant, it can emulsify hydrophobic hydrocarbons,

making it easier to dissolve in water and reducing surface tension. In addition, compared with chemical surfactants, bio-surfactants are less toxic and have higher biodegradability and surface activity [34]. The raw materials for the production of the two surfactants are cheap and easily available, and the production is relatively high. Considering that the porous materials in this article can be used as commercial cleaners in the future, choosing these two surfactants will reduce production costs. The research is of great significance for protecting health, environmental safety and waste utilization.

2 Materials and Methods

2.1 Materials

Mussel shells (genus: *Mytilus* Linnaeus) were obtained from Shengsi, Zhoushan, China. Alkyl polyglucosides (APG, APG2000, 8–10 carbon alkyl chains) and rhamnolipid (RL, 98%) were purchased from Fine Chemical, Shanghai, China. All chemical reagents were of analytical grade. Deionized water was prepared in laboratory. All reagents were prepared with distilled water.

2.2 Preparation of Porous Materials

At room temperature, mussel shells were soaked in 1% HCl solution for 24 h to remove surface stains, and then wash with distilled water until neutral ($\text{pH} = 7$), and then dried at 80°C in oven for 12 h. The mussel shell samples were loaded into a tube furnace and heated to 800°C , 900°C , 1000°C and 1100°C at a rate of $10^\circ\text{C min}^{-1}$ under nitrogen flow at 200 mL/min, respectively. And the calcination step was held for 2 h. Finally, the calcined mussel shells were ground into powder with a mortar and sieved to $< 100\ \mu\text{m}$ mesh particle size, the as-prepared samples were named as CMSP.

2.3 Modification of Shell Powder by Surfactants

2 g CMSP and 1 g alkyl polyglucosides (APG) were completely dissolved in 30 mL deionized water. The solution was transferred into a high pressure reactor, which was heated to 120°C for 24 h. After cooling to room temperature, the obtained composite was rinsed using deionized water, and the composite was dried at 70°C for 8 h in an oven, the obtained sample was named Sample I. The Sample I and 1 g Rhamnolipid (RL) were dissolved in 30 mL deionized water at a high pressure reactor, then heated to 120°C for 12 h, collected and dried the synthetic sample at 70°C use the same method as above. The synthetic sample was denoted as MTAR.

2.4 Characterization

The contact angle was measured by contact angle meter (CA, XG-CAMB, Xuanyichuangxi Industrial Equipment, Shanghai, China) at room temperature with the sessile drop method [35]. The volume of the liquid used was $5\ \mu\text{L}$. All apparent water contact angles were measured three times, and an average value was used. X-ray diffraction patterns (XRD, D/max 2500, Agilent, USA) of samples were recorded by using a powder X-ray diffractometer at a setting of 40 kV and 30 mA. The surface chemical group of the samples was investigated by Fourier transform infrared spectrometer (FTIR, Thermo Fisher Scientific, USA) and X-ray photoelectron spectrometer (XPS, 5000C ESCA System, PHI, USA). The specific surface area and pore-size distribution were performed on Quadrasorb SI instrument (Quantachrome, USA) and calculated with the method of Brunauer-Emmett-Teller (BET). Scanning electron microscopy (SEM, Hitachi S-4800, Tokyo, Japan) was employed to investigate microstructures and morphology of samples.

2.5 Determination of Oil Removal Rate

0.5 g of CMSP and MTAR were put into 20 mL tap water respectively, and used as washing solution. Rapeseed oil and peanut oil were mixed evenly in the ration of 1:1, and spread on the ceramic plate. The ceramic plate was heated in the oven at 40°C for 20 min to make the oil solidify on it. The prepared

ceramic plates were placed in the above washing solutions for 1 min, and shook at a constant speed for 7 min using an oscillator, respectively. Then removed the ceramic plate from the washing solution and dried them. The measurements were repeated three times. The experiment also set a blank control group and a commercially available detergent with tap water. The oil removal rate was calculated use the following formula:

$$D_r = \frac{M_1 - M_2}{M_1 - M_0} * 100\% \quad (1)$$

where M_0 is the quality of the original ceramic plate, M_1 is the quality of the stained ceramic plate, and M_2 is the quality of the washed and dried enamel sheet.

3 Results and Discussion

3.1 Contact Angle Measurement

Fig. 1 shows the contact angles of MTAR samples made from calcined mussel shell powder prepared at different calcination temperatures. The contact angles of MTAR800°C, MTAR900°C, MTAR1000°C and MTAR1100°C were 92.0°, 95.6°, 98.9° and 99.5°, respectively, which were all more than 90°, indicating that the surface of samples were hydrophobic [36]. With the increase of the calcination temperature of mussel shell powder, the contact angle of MTAR samples increased gradually. The reason is that the main component of the mussel shell is calcium carbonate, but it contains a small amount of organic matter. The organic matter will decompose as the temperature rises to form a regular pore structure. The rich pore structure provides a large number of reaction sites for the surfactant and increases its hydrophobicity, so the contact angle is increased [37]. Fig. 2 is the test graph of the contact angle.

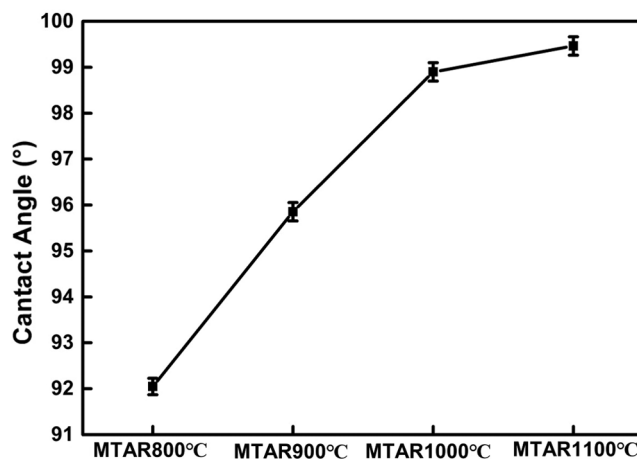


Figure 1: Water contact angle value of as-prepared sample MTAR 800°C, MTAR 900°C, MTAR 1000°C and MTAR 1100°C

But when the temperature reached 1000°C, the increase of contact angle tended to be slow down. This is owing to the high calcination temperature could improve the quality of CaO in the shell. In the subsequent hydrothermal process, CaO is converted into Ca(OH)₂, which increased the content of hydroxide radical in the compound and makes it easier to combined with the APG. In turn, the subsequent assembly with RL is promoted. At the same time, CMSP samples calcined at different temperature were also measured under the same conditions. The contact angle value of calcined mussel shell powder cannot be measured, because its hydrophilicity is too strong. After contact with the sample surface, the water droplets are immediately

absorbed. Considering the material performance and energy saving, MTAR1000°C as the cleaning agent was selected for follow-up experiments.

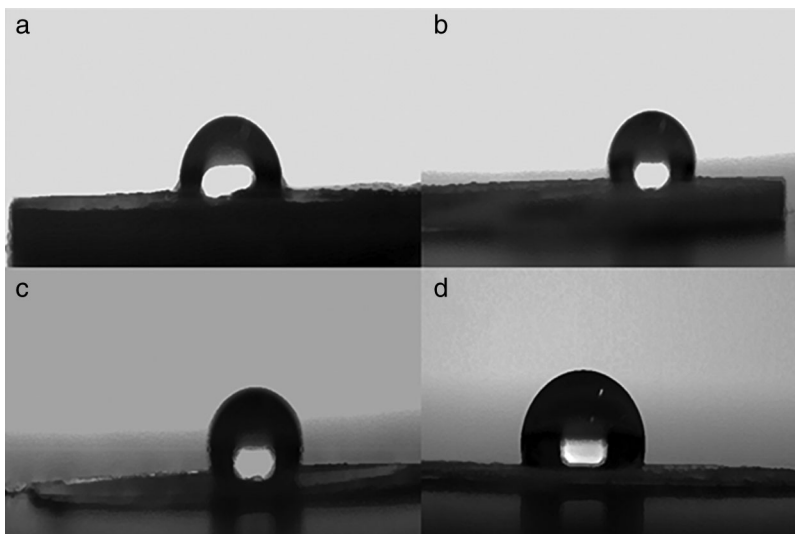


Figure 2: Water contact angle images of as-prepared sample MTAR 800°C (a), MTAR 900°C (b), MTAR 1000°C (c) and MTAR 1100°C (d)

3.2 Characterization of Morphology and Structure

3.2.1 SEM Analysis

SEM photographs of as-prepared samples CMSP1000°C and MTAR 1000°C were shown in Fig. 3. It can be seen from Figs. 3a and 3c that CMSP1000°C has regular layered structure and no obvious pore structure. Comparatively, the texture of MTAR1000°C is loose with a number of relative uniform pores. This indicates that hydrothermal synthesis and surfactant modification [38] plays an active role in the pore formation and its pore size is mainly mesoporous. Because after high temperature pyrolysis, the smooth structure of the raw sample was broken down by devolatilization, condensation, dehydration, and decarboxylation reactions [39].

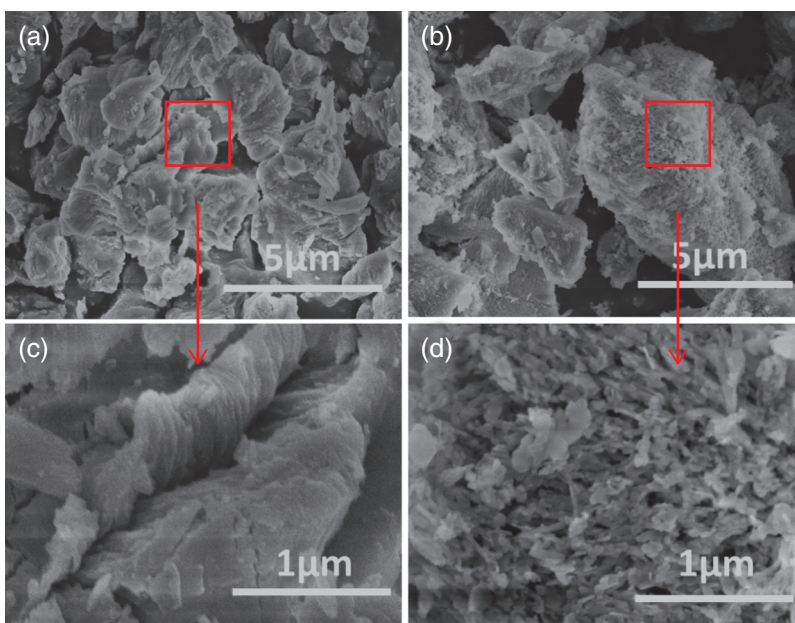


Figure 3: SEM images of samples: (a, c) CMSP1000°C; (b, d) MTAR1000°C

3.2.2 BET Analysis

The specific surface area of two materials was measured via nitrogen adsorption-desorption. Fig. 4 shows two isotherm curves of nitrogen adsorption-desorption, according to the Brunauer classification method, the curves shown in the figure all conform to the standard IV curve and the H3-type hysteresis loops at relative pressure (P/P_0) between 0 and 1.0, which indicates the presence of a mesoporous structure in the sample [40,41]. Tab. 1 shows the calculated BET results of CMSP1000°C and MTAR 1000°C. The specific surface area of the MTAR1000°C and CMSP1000°C is about 49.9 and 2.98 m^2g^{-1} , respectively. The specific surface area after modification by surfactants increased nearly 16.8 times, which confirms that the surfactants (APG and RL) offer more active sites for the oil removal process. It can be seen that the pore sizes are both concentrated in 2–10 nm, which indicates the catalyst includes rich mesoporous.

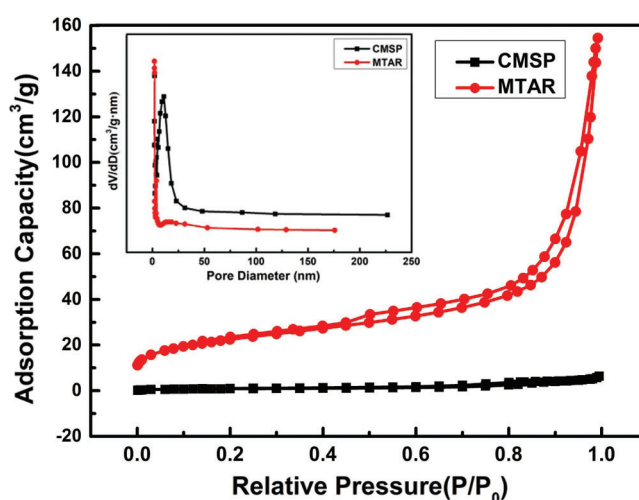


Figure 4: N_2 adsorption-desorption isotherm and pore size distribution of CMSP1000°C and MTAR1000°C

Table 1: The specific surface area and average pore size of different sample

Different sample	CMSP1000°C	MTAR1000°C
Specific surface area (m^2/g)	2.98	49.9
Average pore size (nm)	9.40	9.13
pore volume (cm^3/g)	0.00699	0.114

3.2.3 XRD Analysis

The crystallographic structures of the samples were characterized by X-ray diffraction analysis. As shown in Fig. 5, the as-prepared composites with high crystallinity. The diffraction peaks of CMSP located at $2\theta = 32.20^\circ$, 37.34° and 53.85° , corresponding to the (111), (200) and (220) crystal planes of CaO (JCPDS card number 37-1497). At the same time, the diffraction peaks of MTAR at about $2\theta = 28.66^\circ$, 34.08° , 47.12° , 50.79° and 54.33° could be perfectly indexed to the (100), (101), (102), (110) and (111) crystals planes of $\text{Ca}(\text{OH})_2$ (JCPDS card number 04-0733), respectively. Therefore, the CMSP and MTAR is composed of CaO and $\text{Ca}(\text{OH})_2$, respectively. The calcium carbonate in the mussel shell was decomposed at 1000°C and converted into calcium oxide [42], which was consistent with the

XRD test results. The existence of Ca(OH)_2 crystal in MTAR 1000°C is due to the CaO reacts with H_2O to form Ca(OH)_2 in Teflon-lined autoclave during the hydrothermal process.

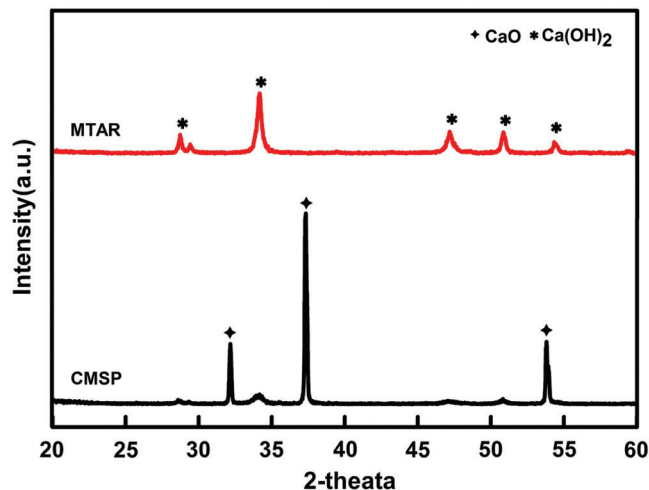


Figure 5: XRD patterns of CMSP 1000°C and MTAR 1000°C

3.2.4 FTIR Analysis

The information on the chemical structure of the samples was investigated by FTIR spectra and corresponding results were shown in Fig. 6. The peak at 876 cm^{-1} was both observed in the two materials, this peak was corresponded to the out-of-plane bending vibration of CO_3^{2-} [43,44]. The peak near 3640 cm^{-1} was observed in the two spectrums of samples, which was owing to the stretching vibration of O-H [45]. The O-H in MTAR may come from hydrothermal synthesis reaction, and APG and RL, because the surface of two surfactants (APG and RL) is rich in O-H groups [46]. The weak peak near 3640 cm^{-1} appeared in CMSP, which may be due to the samples absorbs water from the air. The absorption peak at 2850 cm^{-1} and 2900 cm^{-1} corresponded to the $-\text{CH}_2$ stretching vibration [47]. The absorption peak at 1420 cm^{-1} was corresponded to the C=O stretch from CaCO_3 [46].

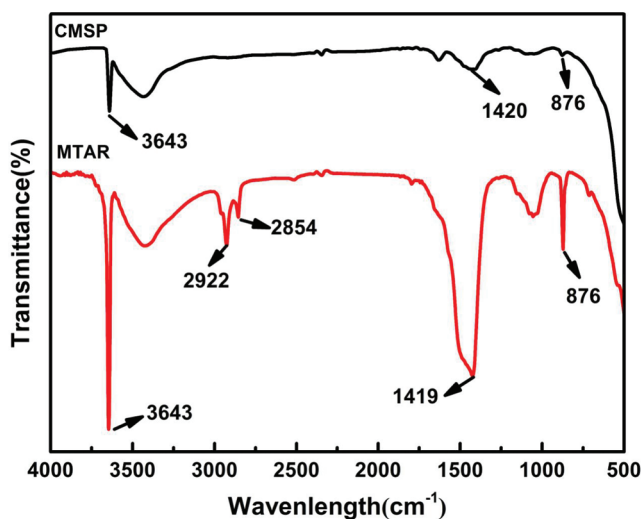


Figure 6: FTIR spectra of CMSP 1000°C and MTAR 1000°C

3.2.5 XPS Analysis

To further determine the surface composition and chemical states of the elements, the as-prepared CMSP and MTAR samples were studied by XPS (Fig. 7a). The survey XPS spectra shows that the CMSP and MTAR contain elements of C, N, O and Ca and the binding energies of C1 s, N1 s, O1 s and Ca2p were at 284.2 eV, 483.2 eV, 531.1 eV and 346.4 eV, respectively. As shown in Fig. 7b, the XPS spectrums of samples were similar, except for the peaks of C1 s. The C1 s high-resolution spectrum of CMSP could be decomposed into three peaks at 288.6 eV (C1), 285.5 eV (C2) and 284.4 eV (C3), which were characteristic of the O-C=O, C-O and the typical carbon atom peak [48–50]. The O-C=O and C-O in the CMSP is mainly from CaCO₃ which is probably derived from Ca(OH)₂ produced by the reaction of CaO in the shell with H₂O and CO₂ in the air [48–50]. In contrast, the C1 s high resolution spectrum of MTAR 1000°C could be decomposed into three peaks at 289.4 eV (C1), 285.3 eV (C2) and 284.8 eV (C3), which correspond to MCO₃ [22], -C-OH and -CH₂- [49], respectively. The peak intensity at 285.3 eV in MTAR may be attributed to the functional groups in APG and RL. Both APG and RL have a large number of -C-OH functional groups [46], so the surfactants were successfully loaded on the surface of calcined shell powder after two self-assembly reactions of hydrothermal synthesis.

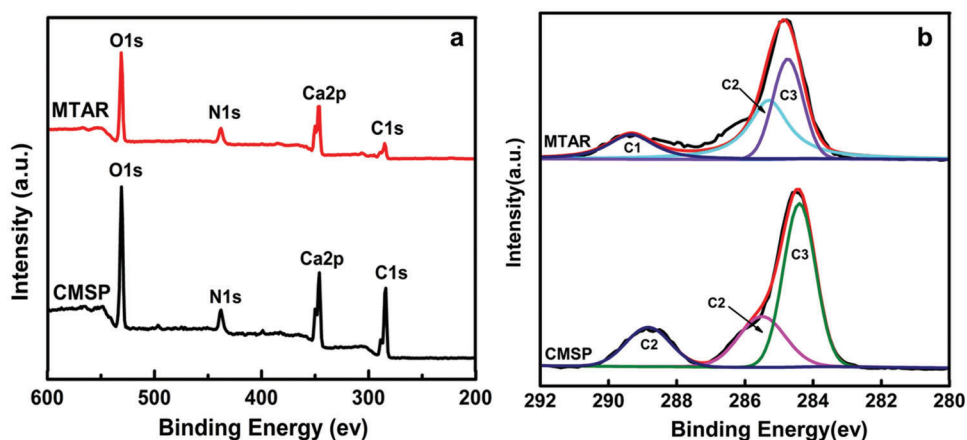


Figure 7: XPS spectra of the CMSP1000°C and MTAR1000°C: (a) survey spectrum, (b) C1 s high-resolution spectrum

3.3 Oil Removal Performance and Mechanism

The washing performance of the as-prepared materials was evaluated by the oil removal rate, and the oil removal rate of series of MTAR and CMSP were shown in Fig. 8. The oil removal rate of surfactant modified samples were extremely high than the unmodified samples. At the same time, the blank control group (tap water) also showed slightly decontamination ability, the oil removal rate was 22.5%, which was caused by the mechanical vibration of the oscillator. As the calcination temperature increased, the decontamination rate of all samples increased. The decontamination rate of CMSP from 800°C to 1100°C is 35.14%, 43.34%, 48.84% and 50.26%. Under the same calcination temperature, the decontamination rate of MTAR is higher than that of CMSP, which is 48.67%, 75.98%, 87.05% and 86.79%, respectively. The oil removal rate values of samples were basically consistent with the contact angle results. In comparison, a commercially available detergent (CAD) was selected for testing, and the decontamination rate was 72.03%.

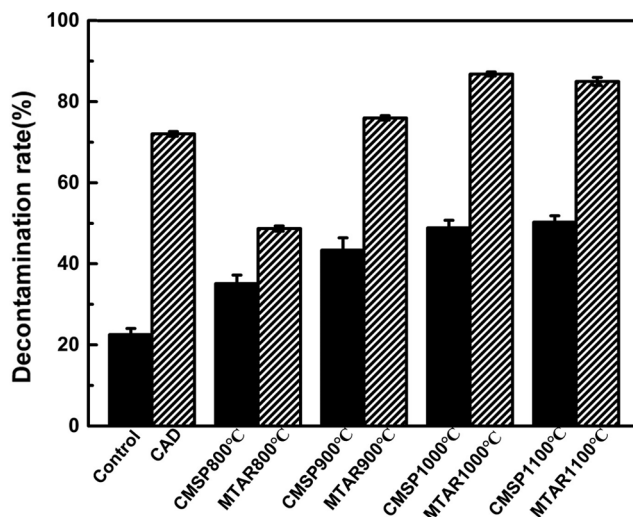


Figure 8: Oil removal rate of shell powder with different treatment methods

As shown in Fig. 9, the oil removal mechanism of as-prepared samples may be that the surfactant on the surface of samples reduces the surface tension of oil, and the pore of samples is used to absorb the oil. At the same time, mechanical vibration is also beneficial to the adsorption and removal of oil. The hydroxyl group of APG is adsorbed on the surface of CMSP in the first step of hydrothermal reaction, and the intermediate product with hydrophilic group on the surface is obtained. MTAR was formed by adsorption of surfactant RL via its hydrophilic groups on the surface of intermediate product, leaving its hydrophobic group outwards. Meanwhile, the surface of the as-prepared MTAR samples exhibited highly porous and dispersive characteristic. The larger specific surface area increases the contact area of the dishwashing detergent with oil, thus improving the oil removal efficiency. In addition, the calcium hydroxide in MTAR can make its aqueous solution have certain alkalinity, which is conducive to the hydrolysis of tableware oil.

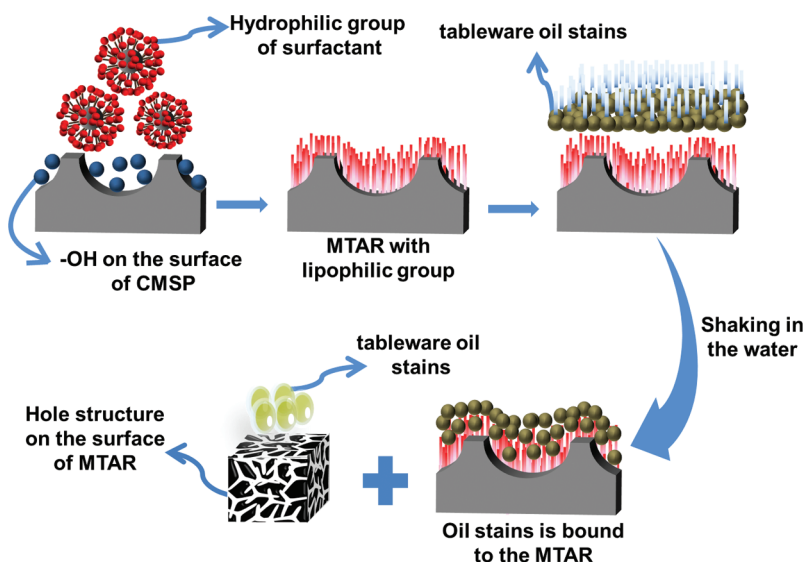


Figure 9: Mechanism diagram of MTAR in the process of removing kitchen oil

4 Conclusions

Novel materials MTAR with excellent removal performance for tableware oil were successfully prepared and synthesized by two-step hydrotherm-assisted synthesis. Compared with CMSP, the surface morphology of MTAR sample is highly dispersive and multihole. After two self-assembly of the surfactant, the surface morphology of the shell powder has undergone great changes, which resulted in the specific surface area increased by 16.76 times. In this work, MTAR 1000°C showed good cleaning ability, the oil removal rate reached 87.05%, which was due to the big specific surface area, loose porous structure and emulsion of surfactants. Particularly, the MTAR is from the organism, which is readily available, renewable and biodegradable materials. This work provides a new idea and method to develop a new kitchen cleaning materials by employing abandoned biomass as raw materials.

Funding Statement: This study was supported by scientific research fund of Zhejiang provincial education department (Y201942627), Zhejiang Provincial Universities and Research Institutes (No. 2019J00025) and Demonstration Project of Marine Economic Innovation and Development of Zhoushan City of China.

Conflicts of Interest: The authors declare that they have no conflicts of interest to report regarding the present study.

References

1. Azizullah, A., Richter, P., Haeder, D. P. (2011). Toxicity assessment of a common laundry detergent using the freshwater flagellate euglena gracilis. *Chemosphere*, 84(10), 1392–1400. DOI 10.1016/j.chemosphere.2011.04.068.
2. Mahalakshmi, R., Pugazhendhi, A., Brindhadevi, K., Ramesh, N. (2020). Analysis of alkylphenol ethoxylates (apeos) from tannery sediments using lc-ms and their environmental risks. *Process Biochemistry*, 97, 37–42. DOI 10.1016/j.procbio.2020.06.015.
3. Wang, Y., Zhang, Y., Li, X., Sun, M., Wei, Z. et al. (2015). Exploring the effects of different types of surfactants on zebrafish embryos and larvae. *Scientific Reports*, 5, 479–483. DOI 10.1038/srep10107.
4. Olkowska, E., Ruman, M., Polkowska, Z. (2014). Occurrence of surface active agents in the environment. *Journal of Analytical Methods in Chemistry*, 2014, 769708. DOI 10.1155/2014/769708.
5. Gloria, E. O., Omolara, T. A., Rufus, O. A., Olaoluwa, S. O., Monica, E. (2020). Assessment of the toxicity and biochemical effects of detergent processed cassava on renal function of wistar rats. *Toxicology Reports*, 7, 1103–1111. DOI 10.1016/j.toxrep.2020.08.007.
6. Abel, P. D. (2010). Toxicity of synthetic detergents to fish and aquatic invertebrates. *Journal of Fish Biology*, 6(3), 279–298. DOI 10.1111/j.1095-8649.1974.tb04545.x.
7. Ezemonye, L. I. N., Ogeleka, D. F., Okieimen, F. E. (2009). Lethal toxicity of industrial detergent on bottom dwelling sentinels. *International Journal of Sediment Research*, 24(4), 479–483. DOI 10.1016/S1001-6279(10)60019-4.
8. Do, D. N., Dang, T. T., Le, Q. T., Lam, T. D., Toan, T. Q. (2019). Extraction of saponin from gleditsia peel and applications on natural dishwashing liquid detergent. *Materials Today: Proceedings*, 18, 5219–5230. DOI 10.1016/j.matpr.2019.07.522.
9. Bersi, G., Vallés, D. P. F., Cantera, A. M., Barberis, S. (2019). Valorization of fruit by-products of bromelia antiacantha bertol: Protease Obtaining and its Potential as Additive for Laundry Detergents. *Biocatalysis and Agricultural Biotechnology*, 18, 101099. DOI 10.1016/j.bcab.2019.101099.
10. Wei, M., Wu, H., Xie, Y., Guo, Y., Cheng, Y. et al. (2017). In vitro anti-microorganism activity and detergency of sapindus mukorossi extract based on surfactive nature. *Journal of the Taiwan Institute of Chemical Engineers*, 80, 1–9. DOI 10.1016/j.jtice.2017.06.015.
11. Ankley, G. T., Burkhard, L. P. (1992). Identification of surfactants as toxicants in a primary effluent. *Environmental Toxicology & Chemistry*, 11(9), 1235–1248. DOI 10.1002/etc.5620110904.

12. Warne, M. S. J., Schifko, A. D. (1999). Toxicity of laundry detergent components to a freshwater cladoceran and their contribution to detergent toxicity. *Ecotoxicology & Environmental Safety*, 44(2), 196–206. DOI 10.1006/eesa.1999.1824.
13. Pettersson, A., Adamsson, M., Dave, G. (2000). Toxicity and detoxification of Swedish detergents and softener products. *Chemosphere*, 41(10), 1611–1620. DOI 10.1016/S0045-6535(00)00035-7.
14. Yao, X. X., Ji, L. L., Guo, J., Ge, S. L., Lu, W. C. et al. (2020). Magnetic activated biochar nanocomposites derived from wakame and its application in methylene blue adsorption. *Bioresource Technology*, 302, 122842. DOI 10.1016/j.biortech.2020.122842.
15. Ma, J. C., Huang, W., Zhang, X. S., Li, Y. C., Wang, N. (2020). The utilization of lobster shell to prepare low-cost biochar for high-efficient removal of copper and cadmium from aqueous: Sorption properties and mechanisms. *Journal of Environmental Chemical Engineering*, 10, 104703. DOI 10.1016/j.jece.2020.104703.
16. Ibrahim, S., Wang, S., Ang, H. M. (2010). Removal of emulsified oil from oily wastewater using agricultural waste barley straw. *Biochemical Engineering Journal*, 49(1), 78–83. DOI 10.1016/j.bej.2009.11.013.
17. Zhao, B. W., Ren, L. Y., Du, Y. B., Wang, J. Y. (2020). Eco-friendly separation layers based on waste peanut shell for gravity-driven water-in-oil emulsion separation. *Journal of Cleaner Production*, 255, 120184. DOI 10.1016/j.jclepro.2020.120184.
18. Xu, R. A., Chen, L., Guo, X., Xiao, Z. H., Liu, R. K. (2018). Biodegradable lignocellulosic porous materials: Fabrication, characterization and its application in water processing. *International Journal of Biological Macromolecules*, 115, 846–852. DOI 10.1016/j.ijbiomac.2018.04.133.
19. Songsaeng, S., Thamyongkit, P., Poompradub, S. (2019). Natural rubber/reduced-graphene oxide composite materials: Morphological and oil adsorption properties for treatment of oil spills. *Journal of Advanced Research*, 20, 79–89. DOI 10.1016/j.jare.2019.05.007.
20. Nwadiogbu, J. O., Ajiwe, V. I. E., Okoye, P. A. C. (2016). Removal of crude oil from aqueous medium by sorption on hydrophobic corncobs: Equilibrium and kinetic studies. *Journal of Taibah University for Science*, 10, 56–63. DOI 10.1016/j.jtusci.2015.03.014.
21. Hu, S., Wang, Y., Han, H. (2011). Utilization of waste freshwater mussel shell as an economic catalyst for biodiesel production. *Biomass and Bioenergy*, 35(8), 3627–3635. DOI 10.1016/j.biombioe.2011.05.009.
22. We, D. Y., Zhang, H. L., Cai, L., Guo, J., Wang, Y. N. et al. (2018). Calcined mussel shell powder (cmsp) via modification with surfactants: Application for antistatic oil-removal. *Materials*, 11(8), 1410. DOI 10.3390/ma11081410.
23. Cai, L., Zhou, Y. R., Wang, Z., Chen, J. L., Liu, J. (2019). Preparation and evaluation of a hierarchical Bi_2MO_6 /MSB composite for visible-light-driven photocatalytic performance. *RSC Advances*, 9(65), 38280–38288. DOI 10.1039/C9RA06559H.
24. Vinu, A., Anandan, S., Anand, C., Srinivasu, P., Ariga, K. et al. (2008). Fabrication of partially graphitic three-dimensional nitrogen-doped mesoporous carbon using polyaniline nanocomposite through nanotemplating method. *Microporous & Mesoporous Materials*, 109(1–3), 398–404. DOI 10.1016/j.micromeso.2007.05.037.
25. Xia, Y. D., Robert, M. (2005). Generalized and facile synthesis approach to N-doped highly graphitic mesoporous carbon materials. *Chemistry of Materials*, 17(6), 1553–1560. DOI 10.1021/cm048057y.
26. White, R. J., Antonietti, M., Titirici, M. M. (2009). Naturally inspired nitrogen doped porous carbon. *Journal of Materials Chemistry*, 19(45), 8645–8650. DOI 10.1039/b911528e.
27. Chandra, V., Yu, S. U., Kim, S. H., Yoon, Y. S., Kim, K. S. (2011). Highly selective CO_2 capture on N-doped carbon produced by chemical activation of polypyrrole functionalized graphene sheets. *Chemical Communications*, 48(5), 735–737. DOI 10.1039/C1CC15599G.
28. Wang, Y. T., Wang, K. Q., Lin, J., Xiao, L. Q., Wang, X. L. (2020). The preparation of nano-mIL-101(Fe)@chitosan hybrid sponge and its rapid and efficient adsorption to anionic dyes. *International Journal of Biological Macromolecules*, 165, 2684–2692. DOI 10.1016/j.ijbiomac.2020.10.073.
29. Cao, B., Yuan, J. P., Jiang, D., Wang, S., Bahram, B. et al. (2021). Seaweed-derived biochar with multiple active sites as a heterogeneous catalyst for converting macroalgae into acid-free biooil containing abundant ester and sugar substances. *Fuel*, 285, 119164. DOI 10.1016/j.fuel.2020.119164.

30. Hu, Y. M., Wang, S., Li, J. C., Wang, Q., He, Z. X. et al. (2018). Co-pyrolysis and co-hydrothermal liquefaction of seaweeds and rice husk: Comparative study towards enhanced biofuel production. *Journal of Analytical and Applied Pyrolysis*, 129, 162–170. DOI 10.1016/j.jaap.2017.11.016.
31. Zhang, F., Gu, W. J., Xu, P. Z., Tang, S. H., Xie, K. Z. et al. (2011). Effects of alkyl polyglycoside (APG) on composting of agricultural wastes. *Waste Management*, 31(6), 1333–1338. DOI 10.1016/j.wasman.2011.02.002.
32. Iglauer, S., Wu, Y. F., Shuler, P., Tang, Y. C., William, A. G. (2009). Alkyl polyglycoside surfactant-alcohol cosolvent formulations for improved oil recovery. *Colloids & Surfaces a Physicochemical & Engineering Aspects*, 339(1–3), 48–59. DOI 10.1016/j.colsurfa.2009.01.015.
33. Markus, M. M., Johannes, H. K., Henkel, M., Gerlitzki, M., Barbara, H. et al. (2012). Rhamnolipids—next generation surfactants? *Journal of Biotechnology*, 162(4), 366–380. DOI 10.1016/j.jbiotec.2012.05.022.
34. Dobler, L., Vilela, L. F., Almeida, R. V., Neves, B. C. (2016). Rhamnolipids in perspective: Gene regulatory pathways, metabolic engineering, production and technological forecasting. *New Biotechnology*, 33(1), 123–135. DOI 10.1016/j.nbt.2015.09.005.
35. Bilal, M., Asgher, M., Iqbal, H. M. N., Hu, H., Zhang, X. (2017). Biotransformation of lignocellulosic materials into value-added products—a review. *International Journal of Biological Macromolecules*, 98, 447–458. DOI 10.1016/j.ijbiomac.2017.01.133.
36. Chen, P., Xie, W. F., Tang, F. Z., Nally, T. M. (2020). Structure and properties of thermomechanically processed chitosan/carboxymethyl cellulose/graphene oxide polyelectrolyte complexed bionanocomposites. *International Journal of Biological Macromolecules*, 158, 420–429. DOI 10.1016/j.ijbiomac.2020.04.259.
37. Simeng, L., Barreto, V., Li, R. W., Chen, G., Hsieh, Y. P. (2018). Nitrogen retention of biochar derived from different feedstocks at variable pyrolysis temperatures. *Journal of Analytical and Applied Pyrolysis*, 133, 136–146. DOI 10.1016/j.jaap.2018.04.010.
38. Li, Y., Wei, Y. N., Huang, S. Q., Liu, X. S., Jin, Z. H. et al. (2018). Biosorption of Cr(VI) onto auricularia auricula dreg biochar modified by cationic surfactant: Characteristics and mechanism. *Journal of Molecular Liquids*, 269, 824–832. DOI 10.1016/j.molliq.2018.08.060.
39. Jian, X. M., Zhuang, X. Z., Li, B. S., Xu, X. W., Wei, Z. B. et al. (2018). Comparison of characterization and adsorption of biochars produced from hydrothermal carbonization and pyrolysis. *Environmental Technology & Innovation*, 10, 27–35. DOI 10.1016/j.eti.2018.01.004.
40. Sing, K. S. W. (1985). Reporting physisorption data for gas/solid systems with special reference to the determination of surface area and porosity (recommendations 1984). *Pure & Applied Chemistry*, 57(4). DOI 10.1351/pac198557040603.
41. Kruk, M., Jaroniec, M. (2001). Gas adsorption characterization of ordered organic-inorganic nanocomposite materials. *Chemistry of Materials*, 13(10), 3169–3183. DOI 10.1021/cm0101069.
42. Fuchs, J., Stefan, M., Schmid, J. C., Hofbauer, H. (2019). A kinetic model of carbonation and calcination of limestone for sorption enhanced reforming of biomass. *International Journal of Greenhouse Gas Control*, 90, 102787. DOI 10.1016/j.ijggc.2019.102787.
43. Masukume, M., Maree, S. O., Jannie, P. M. (2014). Sea shell derived adsorbent and its potential for treating acid mine drainage. *International Journal of Mineral Processing*, 133, 52–59. DOI 10.1016/j.minpro.2014.09.005.
44. Lee, S. W., Jang, Y. N., Ryu, K. W., Chae, S. C., Lee, Y. H. et al. (2011). Mechanical characteristics and morphological effect of complex crossed structure in biomaterials: Fracture mechanics and microstructure of chalky layer in oyster shell. *Micron*, 42(1), 60–70. DOI 10.1016/j.micron.2010.08.001.
45. Krutof, A., Bamdad, H., Hawboldt, K. A., Macquarrie, S. (2020). Co-pyrolysis of softwood with waste mussel shells: Biochar analysis. *Fuel*, 282, 118792. DOI 10.1016/j.fuel.2020.118792.
46. Diana, M., Zdziennicka, A., Bronisaw, J. (2014). Thermodynamic properties of rhamnolipid micellization and adsorption. *Colloids and Surfaces B: Biointerfaces*, 119, 22–29. DOI 10.1016/j.colsurfb.2014.04.020.
47. Chowdhury, S., Saha, P. (2010). Sea shell powder as a new adsorbent to remove basic green 4 (malachite green) from aqueous solutions: Equilibrium, kinetic and thermodynamic studies. *Chemical Engineering Journal*, 164(1), 168–177. DOI 10.1016/j.cej.2010.08.050.

48. Yan, Q., Yang, X. Y., Wei, T., Zhou, C. L., Wu, W. et al. (2019). Porous β -m₂C nanoparticle clusters supported on walnut shell powders derived carbon matrix for hydrogen evolution reaction. *Journal of Colloid and Interface Science*, 563, 104–111. DOI 10.1016/j.jcis.2019.12.059.
49. Zhang, Y. Z., Wang, X. Y., Wang, C. H., Zhai, H. B., Liu, B. S. et al. (2019). Facile preparation of flexible and stable superhydrophobic non-woven fabric for efficient oily wastewater treatment. *Surface & Coatings Technology*, 357, 526–534 DOI 10.1016/j.surfcoat.2018.10.037.
50. Zhang, X. H., Liu, M. H., Kang, Z. W., Wang, B. Q., Wang, B. et al. (2020). Nir-triggered photocatalytic/photothermal/photodynamic water remediation using eggshell-derived CaCO₃/CuS nanocomposites. *Chemical Engineering Journal*, 388, 124304. DOI 10.1016/j.cej.2020.124304.